PHYSICAL REVIEW B **80**, 184418 (2009)

Elastic constants of the single crystalline Yb based heavy-fermion compound $YbCo_2Zn_{20}$

Yoshiki Nakanishi,* Takuya Fujino, Kankichi Ito, Mitsuteru Nakamura, and Masahito Yoshizawa
Graduate School of Frontier Materials Function Engineering, Iwate University, Morioka 020-8551, Japan

Yuta Saiga and Masashi Kosaka
Department of Physics, Saitama University, Saitama 338-8570, Japan

Yoshiya Uwatoko
Institute for Solid State Physics, University of Tokyo, Kashiwa 227-8581, Japan

(Received 12 April 2009; revised manuscript received 1 September 2009; published 18 November 2009)

Ultrasonic measurements have been carried out on the heavy-fermion compound $YbCo_2Zn_{20}$ to investigate the elastic properties and the 4f electric state of Yb ion. A strong temperature dependence at low temperature was found in elastic constants C_{11}, $(C_{11}-C_{12})/2$, and C_{44} of $YbCo_2Zn_{20}$. Furthermore, the elastic constants are significantly magnetic field dependent at low temperatures. These experimental facts strongly suggest an importance of the highly degenerated 4f low-lying level scheme of Yb ions under a crystalline electric field effect, probably leading to such an extremely large Sommerfeld coefficient of $YbCo_2Zn_{20}$. We argue that the near spherical distribution of neighboring Zn atoms centered at the Yb site is an essential requirement for the formation of such an exotic heavy-fermion system.

DOI: 10.1103/PhysRevB.80.184418 PACS number(s): 75.20.Hr, 71.27.+a, 71.70.Ch, 75.30.Mb

I. INTRODUCTION

Much attention has been focused on clathrate compounds and filled skutterudites known as cagelike compounds to discern the nature of the strongly correlated electron system derived from their cage structures.[1–9] Such problems include the interplay between superconductivity, magnetism, multipolar ordering, and heavy fermion (HF) behavior in structurally related materials. In particular, anharmonic vibrations of a guest ion in an oversized cage and strong hybridization between localized f electrons and conduction bands owing to the large number of the cage atom to the guest ion are of central importance in these systems.

A new family of lanthanide intermetallic compounds RX_2Zn_{20} (R=lanthanide and X=transition metal) is one of the ideal candidates for investigating them, as reported previously.[10,11] The RX_2Zn_{20} compounds crystallize in the cubic $CeCr_2Al_{20}$ structure belonging to the space group $Fd\bar{3}m$. A characteristic feature of the crystal structure in these compounds is as follows. The rare-earth ion has the four nearest neighbors as well as the twelve next-nearest neighbors of Zn atoms. Namely, the rare-earth ion is coordinated by a 16 atom Frank-Kasper polyhedron and has a cubic point symmetry.[12,13] It is expected, thus that relatively low crystalline electric field (CEF) split levels are possibly realized due to this near spherical distribution of neighboring Zn atoms.

Thermodynamic and transport properties of YbT_2Zn_{20} manifest strong electric correlations in the HF behavior.[10,11] The intensive investigation of these compounds is certainly motivated by the exceptionally enormous Sommerfeld coefficient γ of 7.9 $J/mol\,K^2$ in $YbCo_2Zn_{20}$, evidenced by the specific-heat measurement. Furthermore, the Sommerfeld coefficient ranges from 500 to 800 $mJ/mol\,K^2$ even in other YbT_2Zn_{20} compounds, which is relatively large compared to that in other Ce-based HF compounds. The temperature-dependent magnetic susceptibility data of $YbCo_2Zn_{20}$ follows well a Curie-Weiss law down to 3 K, confirming the presence of local magnetic moment derived from Yb ion and the low CEF splitting levels. No indications of either magnetic order or superconductivity have been reported so far at low temperatures down to 20 mK.[10] The occurrence of such an enormous γ in $YbCo_2Zn_{20}$ has led to a systematic investigation of magnetic and structural properties of this compound. The origins of the HF properties of $YbCo_2Zn_{20}$ are still unclear. One of the most important and essential issues to elucidate the mechanism, governed the low-temperature properties is to determine the CEF splitting levels.

Elastic constant measurements are particularly well suited to study ground-state properties, via a quadrupolar response of 4f ion and a magnetoelastic interaction. It is because, in general, the coupling of an acoustic strain ε to an ionic quadrupole moment tensor Q is large and the coefficients of the elastic constants depend in a characteristic manner on the components of the charge susceptibility χ_Γ. As described below in detail the elastic constants, as the charge susceptibility, measure the diagonal and off-diagonal quadrupolar matrix elements which correspond to Curie terms and Van Vleck terms in the charge susceptibility, respectively. This is analogous to the magnetic susceptibility which samples the magnetic dipole matrix elements. With a Γ_3 or a Γ_5 quadrupolar-active ground state of the Yb($4f^{13}$) ions one can expect typical quadrupolar effects, especially in the temperature dependence of the elastic constants.

In this paper we present the results of ultrasonic measurements to elucidate the underlying mechanism for the formation of Yb based strongly correlated-electron state observed in $YbCo_2Zn_{20}$, mainly focused our attention on the ground-state properties possibly formed by CEF effect.

II. EXPERIMENTAL DETAILS

Single crystal $YbCo_2Zn_{20}$ was grown in Zn flux. The materials were placed in the ratio Yb:Co:Zn≔1:2:100: in a

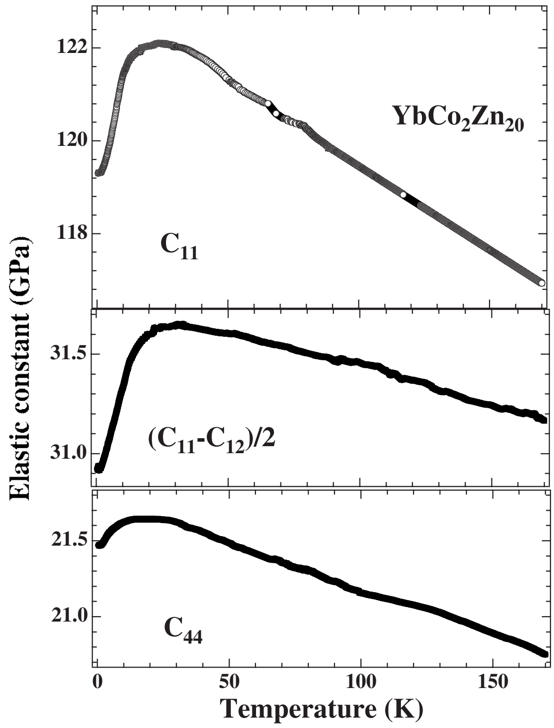

FIG. 1. Temperature dependence of elastic constants C_{11}, $(C_{11}-C_{12})/2$, and C_{44} of $YbCo_2Zn_{20}$.

Ta crucible and sealed under vacuum in a quartz ampoule. Residual Zn flux was etched from the surface of the crystals using diluted HCL or acetic acid. Specimen used for the present ultrasonic measurement was cut into a rectangular shape with two axes along the ⟨001⟩ and ⟨110⟩ directions. The specimen used in our study has a size of $2.5\times3.4\times2.4$ mm^3 with the crystallographic ⟨100⟩ axis directed along the largest dimension.

The sound velocity, as the elastic constant was measured by an ultrasonic apparatus based on a phase comparison method at temperatures down to 0.5 K in magnetic field up to 12 T. Plates of $LiNbO_3$ was used for the piezoelectric transducer. The fundamental resonance frequency of $LiNbO_3$ transducer is 5–30 MHz. The transducer was glued on the parallel planes of the sample by an elastic polymer Thiokol. The absolute value of the sound velocity was obtained by measuring the delay time between the ultrasonic echo signals with an accuracy of a few percent. The elastic constant was calculated as $C=\rho v^2$ by using the sound velocity v and the density ρ of the crystal. The lattice constant of $YbCo_2Zn_{20}$ at room temperature $a=14.15$ Å was used for the estimation of the density $\rho=7.9$ g/cm^3.

III. EXPERIMENTAL RESULTS

We measured the longitudinal as well as transverse ultrasonic velocity. We used 10–30 MHz for the measurement of C_{11} and 5–15 MHz for $(C_{11}-C_{12})/2$ and C_{44}. Figure 1 shows an overview of the longitudinal (C_{11}) and transverse [$(C_{11}-C_{12})/2$ and C_{44}] elastic constants as a function of temperature for the cubic $YbCo_2Zn_{20}$. The absolute values of each elastic constants and calculated bulk modulus $C_B=(C_{11}+2C_{12})/3$ and Poisson ratio $\gamma_P=C_{12}/(C_{11}+C_{12})$ from C_{11} and $(C_{11}-C_{12})/2$ at both 77 and 4.2 K are listed in Table I. These data show normal behavior at higher temperature; a stiffening with decreasing temperature. However, a strong softening was found below around 30 K in the temperature dependence of all modes. The softening for C_{11}, $(C_{11}-C_{12})/2$, and C_{44} amounts to 13%, 11%, and 6%.

TABLE I. The absolute values of each elastic constants and bulk modulus $C_B=(C_{11}+2C_{12})/3$ and Poisson ratio $\gamma=C_{12}/(C_{11}+C_{12})$ at both 77 and 4.2 K.

	Elastic constants	
Mode	at 4.2 K	at 77 K
C_{11}	118.7 GPa	120 GPa
$(C_{11}-C_{12})/2$	30.9 GPa	31.5 GPa
C_{44}	21.5 GPa	21.3 GPa
$C_B=(C_{11}+2C_{12})/3$	77.5 GPa	78.0 GPa
$\gamma=C_{12}/(C_{11}+C_{12})$	0.32(4)	0.32(2)

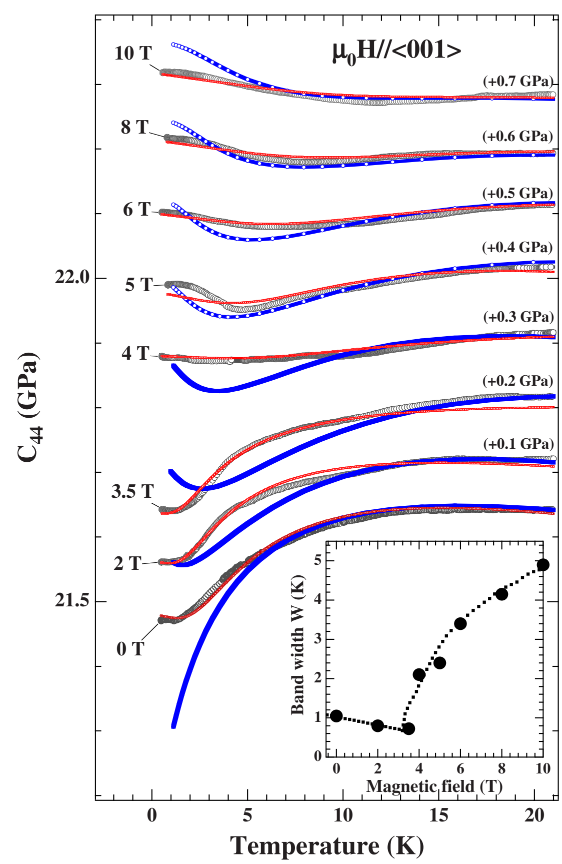

FIG. 2. (Color online) Temperature dependence of elastic constant C_{44} of $YbCo_2Zn_{20}$ in the selected fields. A grayed circle denotes the experimental results. Blue and red lines denote the calculation results based on the formulas (3) and (4), respectively. Inset shows the magnetic field dependence of the bandwidth determined by the results.

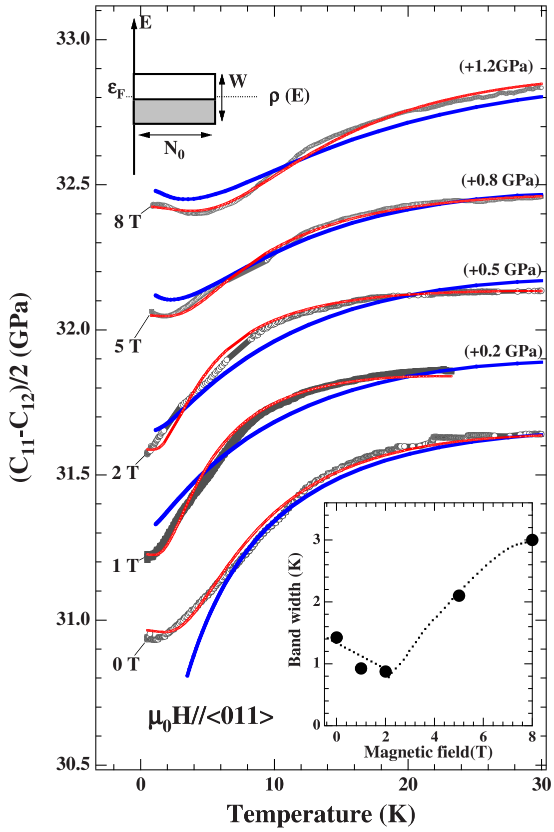

FIG. 3. (Color online) Temperature dependence of elastic constant $(C_{11}-C_{12})/2$ of $YbCo_2Zn_{20}$ in the selected fields. A grayed circle denotes the experimental results. Blue and red lines denote the calculation results based on the formulas (3) and (4), respectively. Insets show the magnetic field dependence of the bandwidth determined by the results (right bottom) and model of a rectangular density of states for a quasiparticle band in $YbCo_2Zn_{20}$ (left top).

A gray circle in Fig. 2 shows the temperature dependence of $(C_{11}-C_{12})/2$ at low temperatures under the selected magnetic fields along $\langle 110\rangle$ axis, offset for clarity in ascending order from bottom to top. The softening below around 30 K becomes suppressed gradually with increasing the magnetic field. It should be noted here that a dip structure at a certain temperature shows up in a field of 3 T. The dip, however, shifts to higher temperatures and becomes smaller as the further increasing magnetic field crosses 4 T and finally undetectable above 5 T.

A gray circle in Fig. 3 shows the temperature dependence of C_{44} at low temperatures under the selected magnetic fields along $\langle 100\rangle$ axis, offset for clarity in ascending order from bottom to top. The softening below around 30 K becomes suppressed gradually with increasing the magnetic field. Also, it is noted here that a dip structure at a certain temperature shows up in a field of 3 T. The dip, however, shifts to higher temperatures and becomes pronounced as the increasing magnetic field above 5 T.

These characteristic behavior will be discussed below in detail, based on the both 4*f*-localized and itinerant electronic state.

IV. ANALYSIS

A. Quadrupolar moment-strain interaction (localized picture)

First, let us discuss elastic anomalies showing up at low temperatures. Characteristic elastic softening toward low temperature, observed in a temperature dependence of the elastic constants is a feature of quantum phenomena. The elastic softening of a localized f electrons system can be usually understood as the quadrupolar response of the system to an external strain associated with a sound wave. The volume strain $\varepsilon_B=\varepsilon_{xx}+\varepsilon_{yy}+\varepsilon_{zz}$ with Γ_1 symmetry associated with a bulk modulus $C_B=(C_{11}+2C_{12})/3$ couples to the Coulomb multipole moment $O_B=O_4^0+5O_4^4$. A softening in C_B is a characteristic phenomena for the valence fluctuation system as SmB_6.[14] In general, C_B increases with decreasing the temperature due to the anharmonicity of the lattice vibration in such compounds with stable 4f electron, and even in the Kondo ones. The elastic strain $\varepsilon_v=\varepsilon_{xx}-\varepsilon_{yy}$ and $\varepsilon_u=(2\varepsilon_{zz}-\varepsilon_{xx}-\varepsilon_{yy})/\sqrt{3}$ associated with the transverse $(C_{11}-C_{12})/2$ mode couples to the quadrupolar moment $O_2^2=J_{xx}-J_{yy}$ and $O_2^0=(2J_z^2-J_x^2-J_y^2)/\sqrt{3}$, respectively with Γ_3 symmetry. On the other hand, the elastic strain ε_{xy} associated with the transverse C_{44} mode couples to the quadrupolar moment O_{xy} with Γ_5 symmetry. These effects have its origin in the modulation of the CEF potential by the strain. The lowest order term of this perturbation can be described by

$$H_{qs}=\sum_i g_\Gamma O_\Gamma(i)\varepsilon_\Gamma. \tag{1}$$

Here, $O_\Gamma(i)$ is the equivalent quadrupolar operator at the ith Yb site and g_Γ (Γ denotes the irreducible representation of the point group, i.e., Γ_3 and Γ_5) is the coupling constant. The scattering of the conduction electrons by the electric quadrupolar moments of 4f electrons leads to a quadrupolar interaction such as the Ruderman-Kittel (-Kasuya) -Yoshida (RKKY) mechanism. This means that the quadrupolar moment $O_\Gamma(i)$ of ith Yb site couples to the moment of the other sites by way of the conduction electrons with the same mechanism as RKKY interaction. This intersite quadrupolar interaction can be described by

$$H_{qq}=\sum_i g'_\Gamma\langle O_\Gamma\rangle O_\Gamma(i). \tag{2}$$

Here, g'_Γ is the quadrupolar coupling constant and $\langle O_\Gamma\rangle$ is the mean field of the quadrupolar moment. The temperature dependence of the symmetric elastic constant C_Γ is described as,[15–17]

$$C_\Gamma(T)=C_\Gamma^{(0)}(T)-\frac{Ng_\Gamma^2\chi_\Gamma^{(s)}(T)}{1-g'_\Gamma\chi_\Gamma^{(s)}(T)}. \tag{3}$$

Here, N denotes the number of Yb ions in unit volume, $C_\Gamma^{(0)}$ and $\chi_\Gamma^{(s)}(T)$ denote the background without quadrupolar-strain interaction and the quadrupolar susceptibility, respectively. In the Yb ion case, the Curie term in the quadrupolar susceptibility due to the Γ_8 state with orbital degeneracy gives rise to the elastic softening proportional to reciprocal temperature at low temperatures in transverse $(C_{11}-C_{12})/2$ mode and C_{44}, whereas the Γ_6 and Γ_7 states have no Curie term, but Van Vleck one in the quadrupolar, resulting in much less elastic softening in both $(C_{11}-C_{12})/2$ and C_{44} mode. This distinctness helps us to determine the $4f$-ground state of rare-earth ion in rare-earth compounds.

B. Deformation potential approximation (itinerant picture)

Second, we discuss the elastic anomalies at low temperatures in the different way apart from the CEF effect. If the system has a large density of states of quasiparticles in the vicinity of Fermi level formed by the hybridization, a coupling between quasiparticles and the relevant elastic strain associated with sound waves becomes significantly strong. This also causes an elastic anomaly at low temperatures. In heavy-fermion compounds, thus, a deformation potential coupling to heavy quasiparticles is of great importance, forming by the strong hybridization between $4f$ states and conduction electron states. In order to explain the elastic softening toward low temperature in $YbCo_2Zn_{20}$, the model of the quasiparticle band is employed. For the simplicity, a rectangular density of states and total bandwidth are assumed as shown in the inset of Fig. 3. In the framework of this model with the assumption, the elastic constant C_Γ may be described by[14,18–22]

$$C_\Gamma = C_\Gamma^0 - \frac{4d^2}{W}\tanh\left(\frac{\beta W}{4}\right), \quad (4)$$

where C_Γ^0 and d denote the background elastic constant and coupling constant, respectively. Here, a rectangular density of states and total bandwidth W are assumed as shown in the inset of Fig. 3.

V. DISCUSSIONS

First, we consider the CEF splitting of the $4f$ level of Yb^{+3} in $YbCo_2Zn_{20}$. The Hund's ground state of multiplet $^5F_3$ in $4f^{13}$ configuration of Yb^{+3} ion is $J=7/2$, which split into Γ_8 quartet, Γ_7 doublet, and Γ_6 doublet under the cubic symmetry. Previous reports on magnetic susceptibility of $YbCo_2Zn_{20}$ shows no deviation from the Curie-Weiss law down to 3 K, indicating that the CEF splitting is significantly small. The blue lines in Figs. 2 and 3 show the calculated results based on the formula (3), where we set the total energy difference $\Delta=0$. Since the explicit level scheme has not yet determined, we cannot conclude the level scheme split by the CEF effect. Nevertheless, the agreement between the experiment and calculation is reasonable in higher magnetic fields, but less in low fields as mentioned above. A deviation between experiment and calculation can be significant in lower magnetic fields if one tries to reproduce a minimum showing up under external magnetic fields based on the formula (3). We cannot obtain the better agreement if we set the other energy difference Δ of 3 K or 5 K, although we do not show them here. The fitting curves as shown by a blue line give us important microscopic parameters such as quadrupolar coupling and intersite quadrupolar interaction constants as follows: $g'_{\Gamma 3}=35.3$ K and $g_{\Gamma 3}=1.07$ K for $(C_{11}-C_{12})/2$ in Fig. 2, and $g'_{\Gamma 5}=30.7$ K and $g_{\Gamma 5}=1.07$ K for C_{44} in Fig. 3.

Second, we would like to discuss the deviation of the experimental results from behavior predicted by the CEF effect in lower fields in more detail. One might speculate about the origin of this deviation due to Kondo effect, reminiscent of the similar behavior observed in $PrFe_4P_{12}$ and $PrInAg_2$.[23–25] Again, our results show the reasonable agreement with calculation based on the cooperative effect of the CEF and Zeeman effect under external magnetic fields, in particular, above 5 T.

Let us then examine the low-field elastic behavior from a different angle. One can obtain better agreement if one applies the deformation potential approximation to reproduce the experimental data in low fields below 5 T, based on the formula (4). A red line in Figs. 2 and 3 shows the theoretical results. As shown in those figures, the calculated results based on the deformation potential are in better agreement with the experimental data, in particular, under low fields than those based on the CEF model as shown in Figs. 2 and 3 by a blue line. On the other hand, the fit based on the deformation potential under high magnetic fields is somewhat difficult to reproduce a minimum showing up around 5 K above a field of 5 T.

Third, we would like to discuss the itinerant and localized nature of $4f$ electrons in $YbCo_2Zn_{20}$. The insets of Figs. 2 and 3 show the magnetic field dependence of the bandwidth estimated by the formula (4) under the condition where the coupling constant d is kept constant, namely, independent of the field. The both of coupling constants d are determined by the elastic constants, $(C_{11}-C_{12})/2$ and C_{44}. The bandwidth changes less below 3 T. However, it increases dramatically above around 3 T with increasing the magnetic field.

An increase in the bandwidth W with increasing magnetic fields suggests a tendency toward the broadening of $4f$ level to gain the Zeeman energy, leading to the suppressed HF behavior. We note that these results are consistent with the recent specific-heat measurements which show the significant suppression of the huge Sommerfeld coefficient γ by the applied field.[26] The suppression of the HF behavior seems to be magnetic sources, probably different from the novel mechanism due to the other ones such as rattling motion, multipolar degrees of freedom discusses energetically in $SmOs_4Sb_{12}$, KOs_2O_6, and $PrFe_4P_{12}$.[27–29] Recently the connection between the formation of heavy-fermion system and the rattling motion are intensively studied both experimentally and theoretically. Since the HF state in $YbCo_2Zn_{20}$ would be destroyed easily by external magnetic field, we suppose that the formation of HF state would not be due to the rattling motion, but magnetic origin. Actually, no ultrasonic dispersion has been observed so far in the frequency range up to 50 MHz in $YbCo_2Zn_{20}$, indicating the absence of rattling motion. Thus, the possible rattling motion of Yb ion in a cage of Zn may be ruled out. Another factor need to be considered is the additional value possibly added to the huge Sommerfeld coefficient γ. It is absolutely difficult to explain such a huge γ value of 7.9 J/mol K^2 in $YbCo_2Zn_{20}$ only by the conventional scenario due to magnetic origin.[30,31]

We naively suggest that these observations point to a possibility that the fluctuation of the quadrupolar moments, consequently and/or the fluctuation of magnetic ones are playing an essential role for the formation of such a huge γ value additionally. Furthermore, a magnetic fluctuation associated with a valence one in Yb ion may play a key and unique role as well in $YbCo_2Zn_{20}$ to form the huge γ value. Anyway our results indicate experimentally that such an anomalous state, probably including a magnetic fluctuation would be suppressed strongly by external magnetic fields within around 3 T. This picture is in good agreement with a small value of Kondo temperature of 3 K in $YbCo_2Zn_{20}$, estimated by previous other measurements.[10]

From these results, thus, we may conclude that the temperature dependence of elastic constants of single crystalline $YbCo_2Zn_{20}$ give indication that quadrupolar effects play a significant role for the temperature-dependent elastic properties of this material. We expect that the quadrupolar interaction constant g' should be strongly reduced possibly due to a growth of quadrupolar fluctuations at low temperatures. As an effect of the application of a magnetic field would reduce the fluctuation, via energy splitting of mostly degenerated $4f$ ground state to gain the Zeeman energy. As a result the softening effects would be recovered reflecting CEF effect under the magnetic fields. It naively suggests here that we speculate that such a huge γ value in $YbCo_2Zn_{20}$ might also be formed by the fluctuation between f and conduction electrons, as pointed out by the recent theoretical studies.[32]

Finally, the results of our measurements add to the experimental indications that there is a critical field of around 3 T, in which the bandwidth W shows a minimum value as shown in the insets of Figs. 2 and 3. We infer that the $4f$ electron system shows a crossover from itinerant nature to localized one at low temperature in $YbCo_2Zn_{20}$. Actually, magnetic field can be one of the efficient control parameters. So far, it is highly nontrivial how the quantum critical point (QCP) is control by applying magnetic field.[33] Nevertheless, the itinerant behavior observed in the present experiment might suggest the valence fluctuation due to the hybridization formed by the $4f$ level located near the Fermi level. Again, this instability with the highly quantum degeneracy seems to be a key mechanism for understanding such a huge γ value in $YbCo_2Zn_{20}$ added to the enhanced effective mass under low fields.

VI. CONCLUDING REMARKS

In this paper we presented the elastic properties of single crystalline $YbCo_2Zn_{20}$. We measured the temperature and field dependences of elastic constants C_{11}, $(C_{11}-C_{12})/2$, and C_{44}. From these experiments we obtain the following conclusions. The highly degenerated orbital degree of freedom, which realized due to the near spherical CEF potential, is responsible for the elastic softening of C_{11}, $(C_{11}-C_{12})/2$, and C_{44} below around 30 K. However, the softening cannot be explained only by the CEF effect under zero and low fields below around 3 T, giving an indication that the quadrupolar moments would be screened significantly, possibly based on the magnetic fluctuation which is associated with quadrupolar moment or/and Yb valence. However, the elastic anomalies would be reproduced reasonably by CEF field effect and Zeeman effect under magnetic fields above around 4 T. We found the characteristic evolution of the bandwidth W which might indicate the crossover from itinerant $4f$ electronic state to localized one. It is indicated and reconfirmed, from this work, that $YbCo_2Zn_{20}$ is a possible candidate for the system being the proximity to a QCP, which would give rise to the novel ground state that the crossover from the itinerant to localized $4f$ state may be realized, being tuned by a magnetic field. In order to check our proposal, microscopic experiments such as neutron diffraction and nuclear magnetic resonance measurements are highly desired. For a further discussion, the same measurements under high pressure are currently in progress.

ACKNOWLEDGMENTS

The measurements have been performed in the Cryogenic Division of the Center for Instrumental Analysis, Iwate University. This work was supported by a Grant-in-Aid for Scientific Research on Innovative Areas "Heavy Electrons" (Grant No. 20102007) of The Ministry of Education, Culture, Sports, Science, and Technology, Japan.

*yoshiki@iwate-u.ac.jp

[1] T. Goto, Y. Nemoto, K. Sakai, T. Yamaguchi, M. Akatsu, T. Yanagisawa, H. Hazama, K. Onuki, H. Sugawara, and H. Sato, Phys. Rev. B **69**, 180511(R) (2004).

[2] Y. Nakai, K. Ishida, K. Magishi, H. Sugawara, D. Kikuchi, and H. Sato, J. Magn. Magn. Mater. **310**, 255 (2007).

[3] N. Ogita, R. Kojima, Y. Takasu, T. Hasegawa, T. Kondo, M. Udagawa, N. Takeda, T. Ikeno, K. Ishikawa, H. Sugawara, D. Kikuchi, H. Sato, C. Sekine, and I. Shirotani, J. Magn. Magn. Mater. **310**, 948 (2007).

[4] K. Kaneko, N. Metoki, T. D. Matsuda, and M. Kohgi, J. Phys. Soc. Jpn. **75**, 034701 (2006).

[5] Y. Nakanishi, T. Tanizawa, T. Fujino, P. Sun, M. Nakamura, M. Yoshizawa, H. Sugawara, D. Kikuchi, and H. Sato, J. Magn. Magn. Mater. **310**, 263 (2007).

[6] Y. Nakanishi, T. Fujino, F. Kikuchi, T. Tanizawa, P. Sun, M. Nakamura, G. Yoshino, A. Ochiai, H. Sugawara, D. Kikuchi, H. Sato, and M. Yoshizawa, J. Phys.: Conf. Ser. **92**, 012072 (2007).

[7] Y. Nemoto, T. Yamaguchi, T. Horino, M. Akatsu, T. Yanagisawa, T. Goto, O. Suzuki, A. Dönni, and T. Komatsubara, Phys. Rev. B **68**, 184109 (2003).

[8] I. Ishii, H. Higaki, S. Morita, M. A. Avila, T. Sakata, T. Takabatake, and T. Suzuki, Physica B **383**, 130 (2006).

[9] Y. Takasu, T. Hasegawa, N. Ogita, M. Udagawa, M. A. Avila, K. Suekuni, and T. Takabatake, Phys. Rev. Lett. **100**, 165503 (2008).

[10] M. S. Torikachvili, S. Jia, E. D. Mun, S. T. Hannahs, R. C. Black, W. K. Neils, Dinesh Martien, S. L. Bud'ko, and P. C. Canfield, Proc. Natl. Acad. Sci. U.S.A. **104**, 9960 (2007).

[11] Y. Saiga, K. Matsubayashi, T. Fujiwara, M. Kosaka, S. Katano,

M. Hedo, T. Matsumoto, and Y. Uwatoko, J. Phys. Soc. Jpn. **77**, 053710 (2008).
[12] V. M. T. Thiede, W. Jeitschko, S. Niemann, and T. Ebel, J. Alloys Compd. **267**, 23 (1998).
[13] T. Nasch, W. Jeitschko, and U. C. Rodewald, Z. Naturforsch., B: Chem. Sci. **52**, 1023 (1997).
[14] S. Nakamura, T. Goto, M. Kasaya, and S. Kunii, J. Phys. Soc. Jpn. **60**, 4311 (1991).
[15] B. Lüthi, J. Magn. Magn. Mater. **52**, 70 (1985).
[16] M. E. Mullen, B. Lüthi, P. S. Wang, E. Bucher, L. D. Longinotti, J. P. Maita, and H. R. Ott, Phys. Rev. B **10**, 186 (1974).
[17] S. Nakamura, T. Goto, Y. Ishikawa, S. Sakatsume, and M. Kasuya, J. Phys. Soc. Jpn. **63**, 623 (1994).
[18] P. Thalmeier, J. Magn. Magn. Mater. **76-77**, 299 (1988).
[19] S. Nakamura, T. Goto, Y. Ishikawa, S. Sakatsume, and M. Kasuya, J. Phys. Soc. Jpn. **60**, 2305 (1991).
[20] P. M. Levy, J. Phys. C **6**, 3545 (1973).
[21] V. Dohm and P. Fulde, Z. Phys. B **21**, 369 (1975).
[22] Y. Nakanishi, M. Oikawa, T. Kumagai, M. Yoshizawa, T. Namiki, H. Sugawara, and H. Sato, Physica B **359-361**, 907 (2005).
[23] Y. Nakanishi, T. Simizu, M. Yoshizawa, T. Matsuda, H. Sugawara, and H. Sato, Phys. Rev. B **63**, 184429 (2001).
[24] Y. Nakanishi, M. Yoshizawa, T. Yamaguchi, H. Hazama, Y. Nemoto, T. Goto, T. D. Matsuda, H. Sugawara, and H. Sato, J. Phys.: Condens. Matter **14**, L715 (2002).
[25] O. Suzuki, H. S. Suzuki, H. Kitazawa, G. Kido, T. Ueno, T. Yamaguchi, Y. Nemoto, and T. Goto, J. Phys. Soc. Jpn. **75**, 013704 (2006).
[26] M. Matsubayashi (private communication).
[27] S. Sanada, Y. Aoki, H. Aoki, A. Tsuchiya, D. Kikuchi, H. Sugawara, and H. Sato, J. Phys. Soc. Jpn. **74**, 246 (2005).
[28] Y. Aoki, H. Sugawara, and H. Sato, Physica B **408-412**, 21 (2006).
[29] K. Sasai, K. Hirota, Y. Nagao, S. Yonezawa, and Z. Hiroi, J. Phys. Soc. Jpn. **76**, 104603 (2007).
[30] C. D. Bredl, S. Horn, F. Steglich, B. Lüthi, and R. M. Martin, Phys. Rev. Lett. **52**, 1982 (1984).
[31] K. Satoh, T. Fujita, Y. Maeno, Y. Onuki, T. Komatsubara, and T. Ohtsuka, Solid State Commun. **56**, 327 (1985).
[32] S. Watanabe, M. Imada, and K. Miyake, J. Phys. Soc. Jpn. **75**, 043710 (2006).
[33] S. Doniach, Physica B & C **91**, 231 (1977).